JOURNAL OF GEOPHYSICAL RESEARCH, VOL. 100, NO. D6, PAGES 11,497–11,508, JUNE 20, 1995

Impact of temperature on oxidant photochemistry in urban, polluted rural and remote environments

Sanford Sillman and Perry J. Samson
Department of Atmospheric, Oceanic and Space Sciences, University of Michigan, Ann Arbor

Abstract. The impact of temperature on formation of O_3 and odd nitrogen photochemistry is investigated using urban-, regional-, and global-scale simulations. Urban and polluted rural environments are explored with a regional simulation derived from a specific episode in the midwestern United States. The simulations predict that O_3 increases with tempera-ture in both urban and polluted rural environments. The O_3-temperature relation is driven largely by chemistry of peroxyacetylnitrate (PAN) which represents an increased sink for both NO_x and odd hydrogen at low temperatures. Isoprene emissions, H_2O, and solar radiation also contribute to the O_3-temperature relation. Possible correlations between temperature and anthropogenic emissions or stagnant meteorology were not included. Observations at urban and rural sites in the United States suggests that O_3 increases with temperature at a faster rate than the models predict. Calculations with a one-dimensional global model suggest that increased temperature in the polluted boundary layer does not lead to increased O_3 in the free troposphere, because increased export of O_3 is balanced by decreased export of odd nitrogen species.

1. Overview

It is widely known that elevated O_3 concentrations in polluted environments are associated with warm temperatures [e.g., *Penner et al.*, 1988; *Vukovich et al.*, 1977; *Clark and Karl*, 1982; *Kelly et al.*, 1986; *Cardelino and Chameides*, 1990]. A variety of factors, including synoptic and boundary layer dynamics, temperature-sensitive emissions, and photochemistry, have been suggested as possible causes for the observed O_3-temperature relationship. Emission of biogenic hydrocarbons increase sharply with temperature [*Lamb et al.*, 1987] and it has recently been suggested that emission rates for anthropogenic volatile organic compounds (VOC) also increase with temperature [Environmental Protection Agency (EPA), 1989; *Stump et al.*, 1992]. Abnormally high temperatures are frequently associated with high barometric pressure, stagnant circulation, and suppressed vertical mixing due to subsidence [*Mukammal et al.*, 1982], all of which may contribute to elevated O_3 levels. The importance of photolysis to the formation of O_3 provides a direct link between O_3 and time of year, and temperature-dependent photochemical rate constants also provide a link between O_3 and temperature [*Sillman et al.*, 1990a; *Cardelino and Chameides*, 1990].

Ramanathan et al. [1987] and *Bruhl and Crutzen* [1988] have recently investigated potential interactions between climate change and photochemistry in the troposphere and stratosphere. *Ramanathan et al.* [1987] discussed the possibility that increased H_2O associated with warmer temperatures could have an impact on tropospheric photochemistry. *Hameed et al.* [1980] and *Callis et al.* [1983] have calculated that tropospheric O_3 would decrease in response to either an increase in temperature and H_2O or a decrease in stratospheric O_3. In either case the decrease in O_3 is associated with an increased source of odd hydrogen via the reaction $O(^1D)+H_2O\rightarrow 2OH$. The predicted decrease is critically dependent on assumed sources of NO_x, which regulates O_3 production and loss in the free troposphere via the reaction $HO_2+NO\rightarrow OH+NO_2$ (leading to production of O_3) and the competing O_3 sink $HO_2+O_3\rightarrow OH+2O_2$. *Bruhl and Crutzen* [1988] predicted increases in northern hemisphere O_3 by a factor of 2 or more over the next 50 years, associated with increased emission of anthropogenic NO_x. These results are all consistent with the notion that there is little direct impact of temperature on O_3 in the free troposphere. However *Sillman et al.* [1990a] have shown that temperature has a direct impact on O_3 in the polluted boundary layer during stagnation events, associated with the temperature-dependent rate of decomposition of peroxyacetylnitrate (PAN).

In this paper we explore the impact of temperature on the photochemistry of O_3, odd nitrogen, and odd hydrogen species in urban and polluted rural environments and implications for the global troposphere. Results are based on simulated photochemistry during a stagnation event in which temperature, H_2O, mixing layer height, photolysis rates, and biogenic VOC emissions are allowed to vary. The simulated relationship between O_3 and temperature is compared with observed O_3-temperature correlations at rural and urban sites in the United States. The photochemical response to temperature is discussed in terms of sources and sinks of the OH radical, which regulates the rate of formation of O_3 in polluted environments. Results suggest that the photochemical response to changes in temperature is driven by several factors, including the reaction rate of PAN, the emission rate for biogenic VOC, photolysis rates, and H_2O concentrations.

Paper number 94JD02146.
0148-0227/95/94JD-02146$05.00

2. Simulation Methods

Results presented here are all based on the photochemical mechanism of *Lurmann et al.* [1986] with modifications

appropriate for conditions in the unpolluted troposphere by *Jacob and Wofsy* [1988]. Reactions of PAN and higher-order homologues with OH, omitted from the Lurmann mechanism but included in most analyses of global-scale photochemistry [Kanakidou et al., 1991; *Kasting and Singh*, 1986] have been added with rates and reaction products equal to those used by *Kasting and Singh* [1986]. The chemistry for isoprene is based on *Paulson and Seinfeld* [1992]. Rates for all reactions have been updated based on recommendations by *DeMore et al.* [1992]. Photolysis rates are calculated for 40° N latitude using methods developed by *Madronich* [1987]. Absorption cross sections, quantum yields, and solar flux data were taken from *DeMore et al.* [1985]. An aerosol optical depth of 0.68 was assumed in simulations for polluted environments, based on turbidity data over the eastern United States [*Flowers et al.*, 1969]. An aerosol optical depth of zero was used in global simulations. Other assumptions included a total O_3 column of 325 Dobson units, surface albedo of 0.15, and single-scattering albedo of 0.75.

Regional-scale processes in polluted environments are based on a model by *Sillman et al.* [1990b] with coarse grid resolution (400x480 km^2, 4° longitude x 5° latitude) and a structure of chemically coherent subgrids designed to incorporate the effect of urban photochemistry. Each 400x480 km^2 region is divided into subregions representing (1) urban plumes within the region, (2) power plant plumes, and (3) rural locations. The urban subregion is represented by the simulation of "generic" urban plumes with emissions equal to the average for all urban sources within the region. Similarly, the power plant subregion is represented by generic plumes with emissions equal to the average for power plant sources. The remaining rural subregion is simulated with emission rates derived from sources that have not been included as urban or power plant sources. Typically, emissions from cities with populations of 50,000 or less that are not part of larger metropolitan areas are entered directly into the rural subregion and larger cities are included in the urban subregion. Each plume is simulated for 12 hours downwind from its source. At the end of the 12-hour period the plume contents are exported to the rural subregion. The model subgrid structure insures that model calculations include photochemistry characteristic of both rural and urban locations and provides a method for estimating the relative impact of rural photochemistry and export from urban and power plant sources on region-wide species concentrations. Tests have shown that that average concentrations within 400x480 km^2 grid boxes calculated with the model agree with results of a higher-resolution (40x40 km^2) model; the two models also give similar results for the 98th percentile values of O_3 [*Sillman et al.*, 1990b].

The vertical structure of the model consists of two layers, a mixed layer with diurnal variation and an entrainment layer. The mixed layer extends from the surface to 150 m at night and increases in height during the daytime up to a specified maximum. The second layer extends from the top of the mixed layer to a fixed maximum, usually equal to the peak height of the mixed layer plus 100 m. Growth of the mixed layer follows the diurnal schedule described by *van Ulden and Holtslag* [1985]. Exchange between layers and with the free troposphere is 0.3 cm s^{-1}, based on estimates for rates of subsidence during stagnant conditions [*Thompson and Lenschow*, 1984]. Surface losses are based on the following deposition velocities: O_3 and NO_2, 0.6 cm; NO, 0.1 cm; HNO_3, 2.5 cm; PAN, 0.25 cm; H_2O_2, 1.0 cm. Emission of anthropogenic species are based on the National Acid Precipitation Assessment Program (NAPAP) inventory, version 5.2, for a typical summer weekday [EPA, 1986]. Diurnal variations in anthropogenic emission rates were also adopted from the NAPAP inventory. Emission rates for isoprene were estimated from the analysis of *Lamb et al.* [1987], which provides rates for different types of vegetation and from data for land use [*Matthews*, 1983]. Sensitivity of isoprene emissions to changes in temperature were also derived from Lamb et al. The diurnal variation of the emission rate for isoprene was taken from the formulation given by *Jacob and Wofsy* [1988]. Horizontal advection between 400x480 km boxes is calculated using second-order moments [*Prather*, 1986].

Results are based on a simulated air pollution event that occurred in the midwestern United States on August 1-2, 1988. The event was characterized by high temperatures (308° K maxima) throughout the midwestern United States and southwest winds of ~3 m s^{-1}. Peak O_3 concentrations at rural sites in Illinois, Indiana, Ohio, and Michigan were 60-80 ppb, which are higher than average but not abnormally high for the region [*Logan*, 1989]. Peak O_3 in excess of 120 ppb was observed at sites in the Detroit, Akron-Youngstown, Cincinnati, Louisville, and Milwaukee metropolitan areas and also at several locations that border Lake Michigan [*EPA*, 1991]. The simulation for this event represented a 1200x1440 km domain bordered approximately by Detroit, Michigan, Atlanta, Georgia, Dallas, Texas, and Omaha, Nebraska over a 4-day period. The model was driven by horizontal wind fields that represent average transport through the mixed layer, calculated by interpolation from observed vertical wind profiles [*Heffter et al.*, 1981]. An afternoon mixed layer height of 1830 m was used based on temperature-height profiles at Flint, Michigan, and analytical methods outlined by *Heffter et al.*, [1981]. Results of this simulation are described in greater detail elsewhere [*Sillman and Samson*, 1993].

A separate simulation for urban-scale photochemistry has been used to analyze the processes that contribute to peak O_3 concentrations. The urban model consists of a conventional horizontal grid with grid spacing either 5x5 km or 20x20 km. Photochemistry, emission rates and vertical structure are the same as in the work of *Sillman et al.* [1990b]. The urban model uses simulated rural species concentrations from the regional model as upwind boundary conditions. Horizontal advection within the urban grid is based on the method of *Smolarkiewicz* [1983]. The urban model has been applied to a specific case, the Detroit metropolitan area, for August 1-2, 1988 [*Sillman and Samson*, 1993]. The Detroit simulation is driven by horizontal winds derived from surface observations in the Detroit metropolitan area on August 1 and 2 [*R. Foltman, Detroit Edison Co., Detroit MI, private communication, 1988*], which are considerably lighter than winds calculated by *Heffter et al.* [1981] (based on vertical soundings at 0600 and 1800 at Flint, Michigan) and used in the regional simulation. Results in this study are based on a 100x140 km model domain with 20x20 km grid resolution.

The 20x20 km grid resolution is generally believed to be inadequate for simulating peak O_3 within an urban area. For the Detroit case used in this study, a comparison has been made between simulations with 20x20 km and with 5x5 km resolution. Results of this comparison showed that peak O_3 is

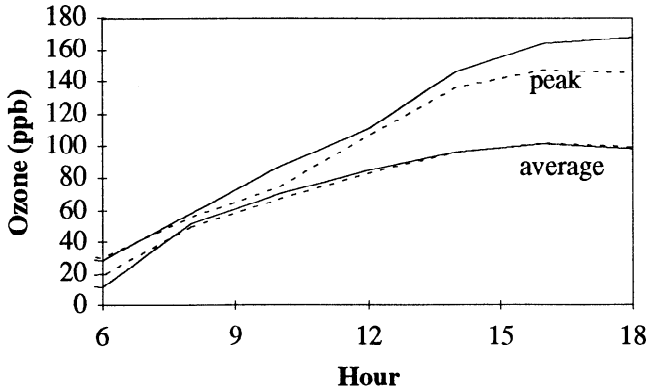

Figure 1a. Simulated average and peak O_3 concentrations (ppb) in the Detroit metropolitan area for August 2, 1988 based on three-dimensional Eulerian models using 5x5 km grid resolution (solid curves) and 20x20 km grid resolution (dotted curves).

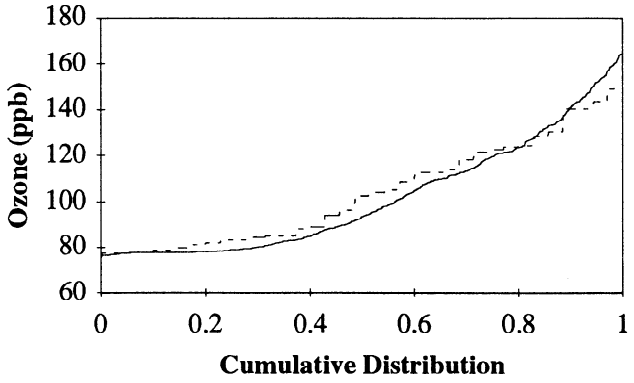

Figure 1b. Simulated distribution of O_3 (ppb) within the Detroit metropolitan area for August 2, 1988, based on three-dimensional Eulerian models using 5x5 km grid resolution (solid lines) and 20x20 km grid resolution (dotted lines).

significantly higher when 5x5 km resolution is used (162 ppb versus 148 ppb with 20x20 km resolution). The change in grid resolution had little impact (<2%) on average O_3 or on the distribution of O_3 within the model domain (see Figure 1). This contrasts with the results of *Sillman et al.* [1990b] which showed that simulated average concentrations are sensitive to grid resolution for grids of 40x40 km or larger. The remainder of this study is based on results from the initial 20x20 km model, which we believe is adequate for illustrating sensitivity to temperature in urban environments.

Global impacts are analyzed with a one-dimensional model for the northern hemisphere adopted from the tropospheric component of *Bruhl and Crutzen* [1988]. The model consists of nine vertical layers and extends from the surface to 20 kPa. The lower two layers are divided into subgroups representing the polluted and remote boundary layer, a distinction similar to the "chemically coherent regions" developed by *Thompson et al.* [1990]. The polluted subregion is further divided into subsections representing rural, urban, and power plant plumes as in the regional model described above. Anthropogenic emission rates for NO_x and VOC in the polluted subregion and partitioning among rural, urban, and power plant subsections are based on average emission rates for eastern North America, as reported by the NAPAP inventory. Global emission rates for NO_x and CO, including both anthropogenic and natural sources, are based on estimates by Bruhl and Crutzen with modifications to represent rates for the northern hemisphere. Anthropogenic emissions are entered entirely in the polluted subregion. The volume of the polluted subregion is equal to 3.9% of the global volume of each vertical layer, a figure determined by dividing the total anthropogenic NO_x source by the emission rate per unit area in the polluted region. Emission of isoprene is based on a global estimate of 400 Tg per year [*Dignon and Logan*, 1990]. The diurnal average emission rate for isoprene in the polluted subregion is $9x10^{10}$ molecules cm^{-2} s^{-1}, equal to the estimate for eastern North America at 303° K derived from *Lamb et al.* [1987] and *Matthews* [1983]. The emission rate in the remote troposphere is $2.2x10^{10}$ molecules cm^{-2} s^{-1}. Emission of VOC other than isoprene in the remote subregion is zero.

Vertical transport is based on eddy diffusion coefficients presented by *Bruhl and Crutzen* [1988]. Net flux at the top of the model domain is equal to the flux estimates by *Logan* [1985] for NO_x and by *Fishman and Crutzen* [1977] for O_3. HNO_3, and H_2O_2 are removed by wet deposition at a rate of $2.4x10^{-6}$ s^{-1} at altitudes of 6 km and below, decreasing to $4.0x10^{-7}$ s^{-1} above 10 km [*Kasting and Singh*, 1986]. Temperatures are based on the U.S. Standard Atmosphere. A 50% relative humidity is assumed throughout the troposphere. The model is exercised for a 4-month time period with a diurnal cycle and photolysis rates for 40°N calculated as described above.

3. Results of Urban and Regional Simulations

The urban and regional simulations were repeated for maximum surface temperatures extending from 308°K, corresponding closely to observed conditions, to 268°K. Emission of isoprene was varied based on the isoprene-temperature relationship reported by *Lamb et al.* [1987]. Additional simulations were performed with isoprene emissions held constant at values calculated for 308°K (=$9x10^{10}$ molecules cm^{-2} s^{-1} diurnally and spatially averaged) and for 293°K (=$2x10^{10}$ molecules cm^{-2} s^{-1}). Photolysis rates were varied according to season with summer corresponding to 298°-308°K, fall corresponding to 283°-293°K, and winter corresponding to 268°-278°K. Wind speeds and mixed layer heights were unchanged in the simulations, although we expect that winter conditions will be associated with higher wind speeds and lower mixed layer heights [*Holtzworth*, 1974]. This exercise is similar to the one reported by *Cardelino and Chameides* [1990] for Atlanta, extended to include rural photochemistry and regional transport.

Simulated peak O_3 concentrations in rural Michigan from the regional simulation and peak Detroit area O_3 from the urban simulation are shown in Figure 2. Both rural and urban O_3 increase as temperature increases from 283° to 308°K. Below 283°K, O_3 remains constant at near-background concentrations. The sharpest rise in O_3 is associated with the switch from fall to summer photolysis rates. The increase in O_3 associated with high versus low isoprene emissions is actually greater in the urban model than in the rural subgrid, despite the fact that isoprene is smaller as a percentage of total VOC in urban locations. We attribute this to the greater sensitivity of urban photochemistry to VOC concentrations.

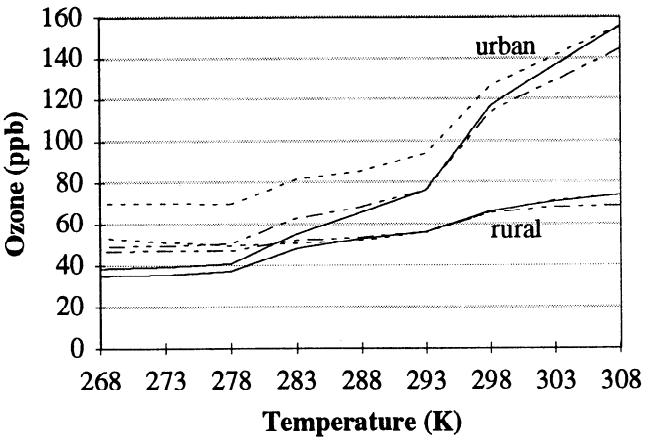

Figure 2. Simulated peak O_3 (ppb) versus maximum temperature (K) in rural Michigan and in the Detroit metropolitan area, based on meteorological conditions for July 30 to August 2, 1988. Results are from simulations with temperature-dependent emissions of isoprene (solid line) and with isoprene emission profiles fixed at values appropriate for 308 K (dotted line) and 293 K (dashed-dotted line).

The subgrid structure of the regional model allows a rough analysis of the relative contributions of photochemistry in urban plumes, power plant plumes and rural areas to regional O_3, by summing volume-weighted ozone production and loss in each model subsection throughout the simulation. Results (Figure 3) show that O_3 production in urban and power plant plumes drops sharply with decreasing temperature and the plumes become net sinks for O_3 at temperatures below 288°K. Rural O_3 production also decreases with temperature but at a slower rate and the significant decrease in rural production (at 283°K) is associated with the switch to winter photolysis rates. Rural photochemistry accounts for greater total production of O_3 than photochemistry in urban or power plant plumes, although peak concentrations are higher in urban plumes.

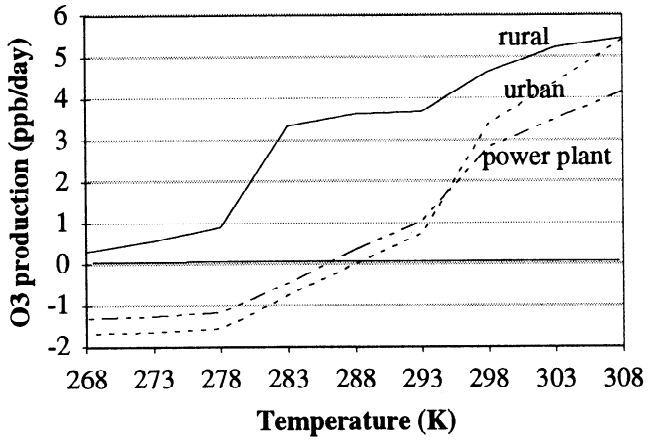

Figure 3. Net photochemical production of O_3 weighted by volume as a percentage of the total model domain (ppb d^{-1}) associated with model subregions representing urban plumes, power plant plumes, and locations not affected by plumes from major sources, versus maximum temperature (K), from a simulation for the midwestern and southeastern United States.

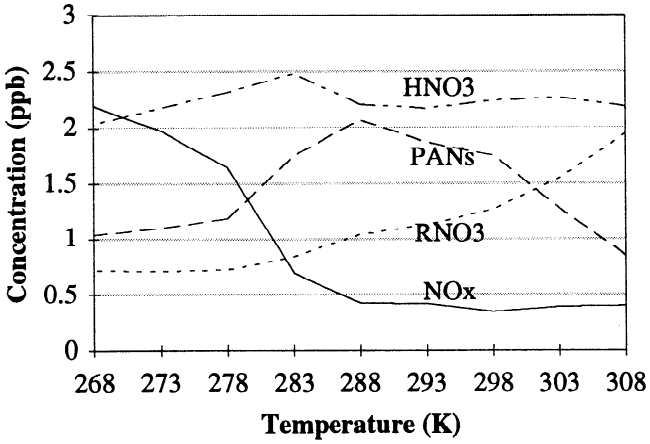

Figure 4a. Simulated NO_X, PANs, HNO_3 and RNO_3 (ppb) at 1400 versus diurnal maximum temperature (K) in rural Michigan, based on the meteorology of August 2, 1988.

Simulated concentrations of nitrogen-containing species in rural Michigan at 1600 are shown in Figure 4a. Concentrations of PANs (including PAN and other species with the form RCO_3NO_2, with PAN accounting for approximately 2/3 of the total) decrease as temperatures increase from 288 to 308, due to the decrease in lifetime at higher temperatures and despite the increase in isoprene. The increase in alkyl nitrates between 298° and 308°K is associated with increasing isoprene. Alkyl nitrates are predicted to be the dominant nitrogen-containing species in rural Alabama, a region with low anthropogenic emissions and high isoprene (Figure 4b). The simulated high alkyl nitrates are much higher than observed in rural Pennsylvania [*Buhr et al.*, 1990], suggesting possible errors either in alkyl nitrate yields (~10% from both >C3 alkanes and isoprene) or in photochemical lifetimes. NO_X is predicted to account for less than 40% of total NO_Y although NO_X becomes more important at low temperatures. Simulations with mixed layer heights reduced to 900 m, appropriate for winter conditions, predict higher NO_X but still less than 50% of afternoon NO_Y (Figure 4c).

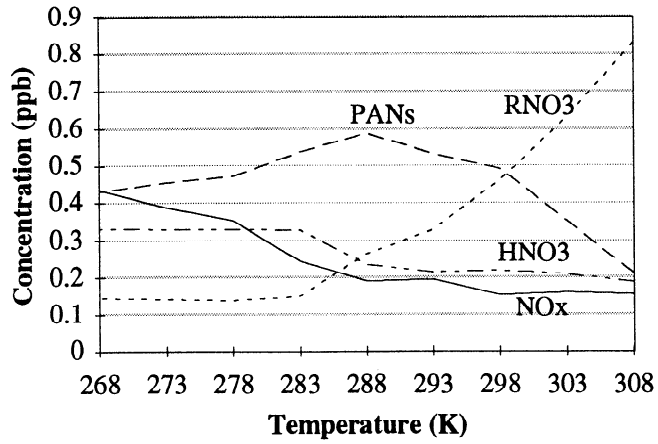

Figure 4b. Simulated NO_X, PANs, HNO_3 and RNO_3 (ppb) at 1400 versus diurnal maximum temperature (K) in rural northern Alabama, based on the meteorology of August 2, 1988.

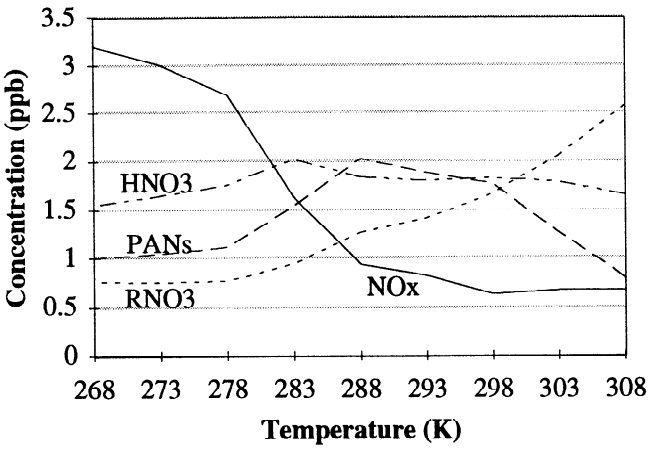

Figure 4c. Simulated NO_x, PANs, HNO_3 and RNO_3 (ppb) at 1400 versus diurnal maximum temperature (K) in rural Michigan with the afternoon mixed layer height reduced to 900 m.

Odd hydrogen species (Figure 5) drop with decreasing temperature due to decreasing H_2O and O_3 photolysis rates. The change in OH/HO_2 ratios with temperature is associated with changed VOC/NO_x ratios and, in particular, with temperature-sensitive emission of isoprene. The seasonal dependence of H_2O_2, evident in Figure 5, has been discussed by *Kleinman* [1991] and Jacob et al. [1995].

The response to decreasing temperature of O_3, nitrogen-containing species, and odd hydrogen in these simulations can be attributed to a combination of four factors: reduction in photolysis rate at low temperatures (associated with season), reduction in water vapor concentration with decreasing temperature, reduction in emission of isoprene, and reduction in the rate of chemical decomposition for PAN and its homologues. The impact of each of these factors has been explored by repeating the original simulation at 308°K with parameters associated with each factor changed to the value appropriate for 293°K, e.g. with isoprene emission rate or PAN decomposition rate equal to the 293 °K value. Concentrations of O_3, odd hydrogen, and nitrogen-containing species in rural Michigan and in Detroit from these test simulations are shown in Table 1. As shown, simulations with parameters associated with all four factors set to 293°K values show little difference from the original simulation for 293°K. Thus changes in rates of other reactions associated with the change from 308°K to 293°K have negligible impact.

Results for rural Michigan suggest that changes in O_3 are mainly associated with the rate of PAN decomposition. The simulation with the PAN decomposition rate equal to the 293°K value and all other parameters at values for 308°K ("308p" in Table 1) yields an O_3 concentration even lower than in the original 293°K simulation. Concentrations of OH, HO_2, NO_x, and PAN are affected by the other temperature-dependent factors as well as by the PAN rate. Odd hydrogen species increase when sources of odd hydrogen ($O(^1D)+H_2O$ and isoprene reactions) increase.

The reason for the decline in O_3 associated with PAN decomposition is that PAN apparently represents a major sink for NO_x in rural environments. As shown in Table 1, the simulated afternoon concentration of NO_x drops by half (from 0.4 to 0.2 ppb) when the PAN decomposition rate is changed from the 308° to the 293° K value. The causal link between PAN decomposition, NO_x concentration, and rural O_3 is partially masked because changes in sunlight and H_2O also affect the concentration of NO_x. Referring to Table 1, a decrease in sunlight and H_2O directly causes a decrease in OH and HO_2. The photochemical lifetime of NO_x is lengthened and the NO_x concentration rises, but the product HO_2*NO_x associated with the odd-oxygen-producing reaction $HO_2+NO->NO_2+OH$ does not change significantly. By contrast, when the rate of PAN decomposition is decreased, NO_x drops sharply, while OH and HO_2 remain largely unaffected. Consequently, the rate of the important HO_2+NO reaction shows a substantial decrease. The photochemical response in an urban environment is fundamentally different, although the final result, a decrease in O_3 with temperature, is similar. As shown in Table 1, the change in the PAN decomposition rate accounts for half of the decrease in O_3, with the remaining decrease due primarily to sunlight and H_2O.

We attribute the impact of PAN in urban environments to its role as a sink for odd hydrogen, in addition to its impact on NO_x as suggested by *Cardelino and Chameides* [1990]. Referring to Table 1, the change in the PAN decomposition rate associated with temperature (308p versus 308) causes 20-30% reductions in OH, HO_2, and NO_x, with reduced production of O_3 resulting the simultaneous decrease of HO_2 and NO. However, the analogous change in PAN decomposition between 308iw and 308iwp causes an increase in NO_x in combination with increased PAN, decreased OH, HO_2, HNO_3, and O_3. In this situation the impact of increased PAN must be associated with its role as a sink for odd hydrogen rather than as a NO_x sink. NO_x increases because the reduced formation rate for HNO_3, associated with the drop in OH, more than compensates for increased PAN. Reduced solar radiation, water vapor, and isoprene all cause additional decreases in OH, HO_2, and O_3, increases in NO_x, and decreases in the product $[HO_2][NO]$ associated with ozone production. This type of behavior is characteristic of VOC-sensitive rather than NO_x-sensitive photochemistry. VOC-sensitive regimes occur when the NO_x source exceeds the chemical source of odd hydrogen (see discussion by *Kleinman* [1991]). Production of O_3 and

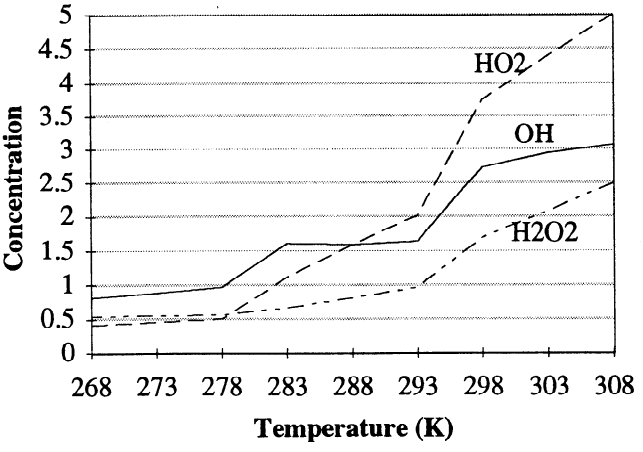

Figure 5. Simulated OH (10^6 molecules cm^{-3}), HO_2 (10^8 molecules cm^{-3}), and H_2O_2 (ppb) at 1400 versus diurnal maximum temperature (K) in rural Michigan, based on the meteorology of August 2, 1988.

Table 1. Species Concentrations at 1400 From Simulations With Modified Assumptions

Simulation	O_3 ppb	OH 10^5mol cm^{-3}	HO_2 10^5mol cm^{-3}	NO_x ppb	PANs ppb	HNO_3 ppb	RNO_3 ppb
			Rural Michigan				
308	74	3.1	5.0	0.4	0.8	2.2	1.9
308iw	66	2.1	2.5	0.7	0.4	2.9	1.0
308p	48	1.9	4.1	0.2	3.0	1.1	1.8
308ip	53	3.0	4.3	0.3	1.9	2.1	0.9
308iwp	54	1.6	2.2	0.5	1.9	2.1	1.0
293	56	1.6	2.0	0.4	1.9	2.2	1.1
			Detroit				
308	154	4.7	8.6	2.9	5.4	9.4	4.4
308iw	102	1.8	1.2	9.4	1.7	8.4	2.8
308p	112	3.2	6.6	1.9	10.6	6.3	4.3
308ip	107	3.9	4.9	2.8	8.6	8.2	3.4
308iwp	75	1.1	0.5	10.5	3.8	6.3	2.5
293	76	1.1	0.4	10.7	3.7	6.4	7.7

Simulations represent the base case with maximum temperature 308 K, 293 K, and 308 K with various parameters changed to values from 293 K simulation. 308, simulation with diurnal maximum temperature 308 K; i, simulation with emission rate for isoprene changed to value for temperature 293 K; w, simulation with autumn photolysis rates and water vapor reduced to value for temperature 293 K; p, simulation with PAN decomposition rate changed to value for temperature 293 K; 293, simulation with diurnal maximum temperature 293K.

photochemical removal of NO_x are both limited by the availability of odd hydrogen, and NO_x is either removed by export (in urban locations) or accumulates (in the Arctic winter).

Trainer et al. [1993] reported a consistent correlation between measured O_3 and NO_x reaction products (NO_y-NO_x) at rural sites in eastern North America, with the ratio $\frac{O_3 - 35\ ppb}{NO_y - NO_x} = 8.5$ and uncertainty (estimated here based on one standard deviation in the reported measurements) ± 3. These correlations were based on photochemically aged air and summer conditions in a year [1988] marked by unusually warm temperatures. The equivalent ratio for the simulated rural locations shown in Figures 2 and 4 varies from 7.5 at 308° K to 5.0 at 293° K, with the ratio at high temperatures consistent with the range of values reported by *Trainer et al.* [1993]. The equivalent ratio for simulated peak O_3 in Detroit, Table 1, drops from 6.0 at 308° K to 4.7 at 293° K. The impact of temperature on the ratio is less in the urban case, also reflecting the difference between urban and rural chemistry. The ratio drops to very low values (<1) in simulations with temperature and solar radiation representative of winter conditions.

4. Comparison With Observations

The observed relation between O_3 and temperature has been derived at a number of urban and rural sites in the United States. Measured concentrations of O_3 have been obtained from the monitoring network of the *EPA* [1991] and temperatures from the National Weather Service for the period April 1 to September 31, 1988. Diurnal peak O_3 is plotted against diurnal maximum temperature at several sites in Figures 6a-f. For urban locations, e.g., New York City, peak

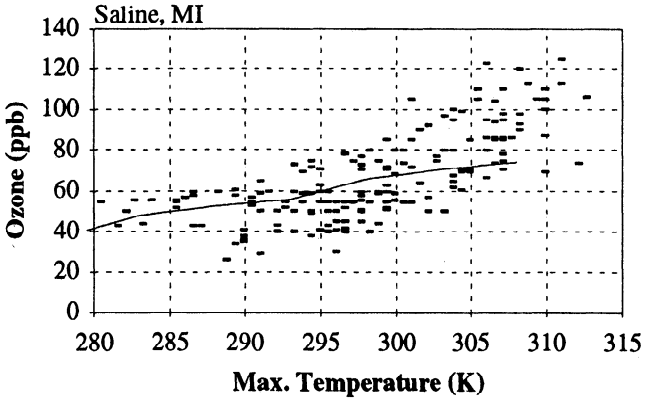

Figure 6a. Diurnal peak O_3 (ppb) at Saline, Michigan versus maximum temperature for April 1-September 30, 1988, based on measurements from *EPA* [1991]. The solid line represents simulated O_3 versus temperature (Figure 2a).

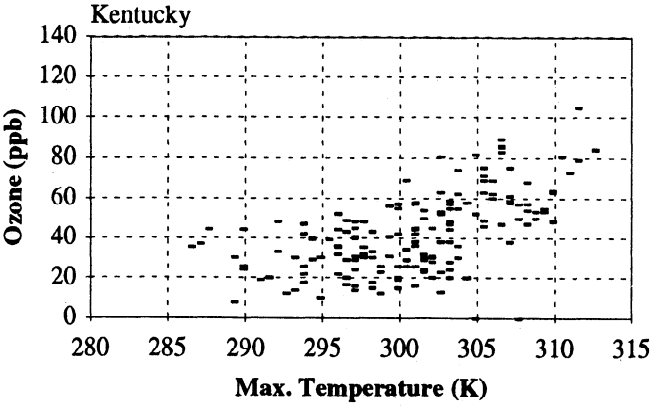

Figure 6b. Diurnal peak O_3 (ppb) in rural Kentucky versus maximum temperature for April 1 to September 30, 1988, based on measurements from *EPA* [1991]. Points represent the lowest diurnal maximum value from a network of 15 sites.

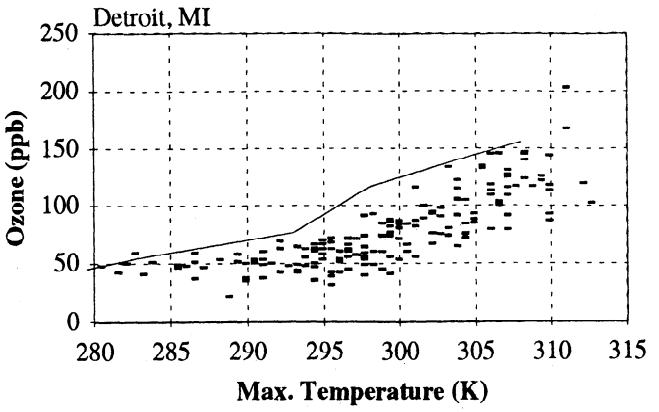

Figure 6c. Diurnal peak O_3 within the Detroit metropolitan area (ppb) versus maximum temperature for April 1 to September 30, 1988, based on measurements from *EPA* [1991]. The solid line represents simulated O_3 versus temperature (Figure 2a).

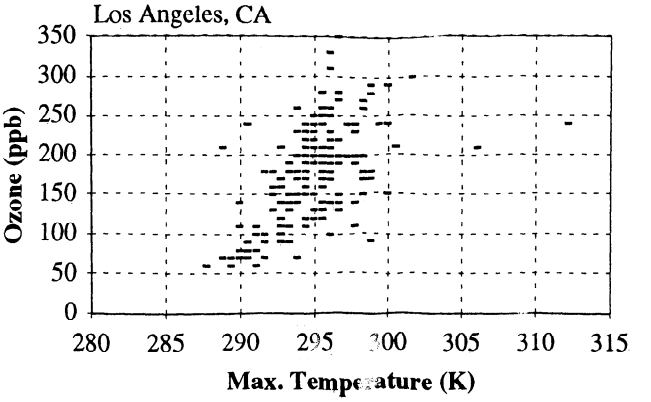

Figure 6e. Diurnal peak O_3 (ppb) in southern California versus maximum temperature at Los Angeles for April 1 to September 30, 1988, based on measurements from *EPA* [1991].

O_3 represents the observed maximum from sites throughout the metropolitan area. Plots for rural locations represent diurnal maximum O_3 at a single site. However, in one case (Kentucky), the value for O_3 has been taken as the lowest diurnal peak O_3 recorded at all monitoring sites within the state. This lowest-peak O_3 is more likely to represent rural conditions, whereas O_3 at an individual rural site can be affected by transport from local sources of emissions.

The observed O_3-temperature relation shows a similar pattern at urban and rural sites in the eastern half of the United States. O_3 concentrations remain low at low temperatures and consistently increase with increasing temperature for temperatures in excess of 300 K. A statistical regression has been performed on the paired O_3-temperature data and separate slopes derived for temperatures above and below 300° K (Table 2). Results show that for T>300° K, the O_3-temperature relationship is statistically significant at all sites. The rate of increase is 3-5 ppb per K at rural sites and ranges from 4 to 9 ppb per K at the three eastern urban sites (New York, Detroit and Atlanta). The lowest-peak O_3 in Kentucky is lower than peak O_3 at individual rural sites, including those in Kentucky, by ~20 ppb, but shows the same dependence on temperature.

Two western sites, Williston, North Dakota and Billings, Montana, show a much weaker dependence on temperature, possibly reflecting the lower level of anthropogenic activity. A third western site, Medford, Oregon, shows an O_3-temperature relationship comparable to rural eastern sites. The O_3-temperature relationship in southern California is complicated by the fact that temperatures vary greatly within the region. We have plotted peak O_3 within the region against temperature at Los Angeles International Airport, a marine location which rarely sees temperatures above 300° K. The result shows a strong link between O_3 and temperature for temperatures between 290° and 300° K, comparable to the O_3-temperature relationship for T>300° K at other cities.

Correlations between peak O_3 and temperature have also been recorded by *Wunderli and Gehrig* [1991] for three locations in Switzerland. At two sites near Zurich they found that peak O_3 increases 3-5 ppb K^{-1} as diurnal average temperature increases from 283° and 298° K, and that peak O_3 does not change as temperatures vary between 273° and 283° K. At the third site, a high-altitude location removed from anthropogenic influence, there was much less variation of O_3 with temperature.

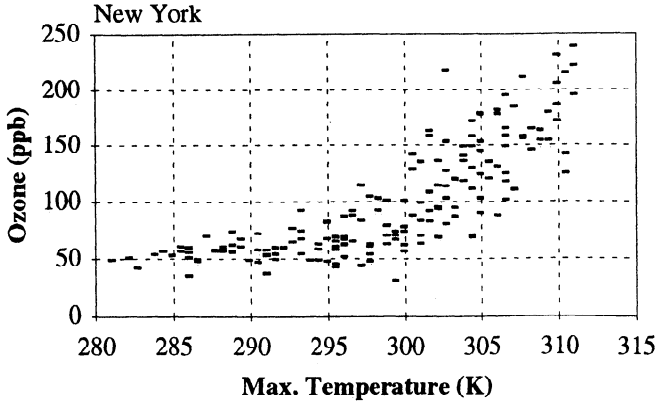

Figure 6d. Diurnal peak O_3 (ppb) versus maximum temperature observed in the New York-New Jersey-Connecticut metropolitan region for April 1 toSeptember 30, 1988, based on measurements from *EPA* [1991].

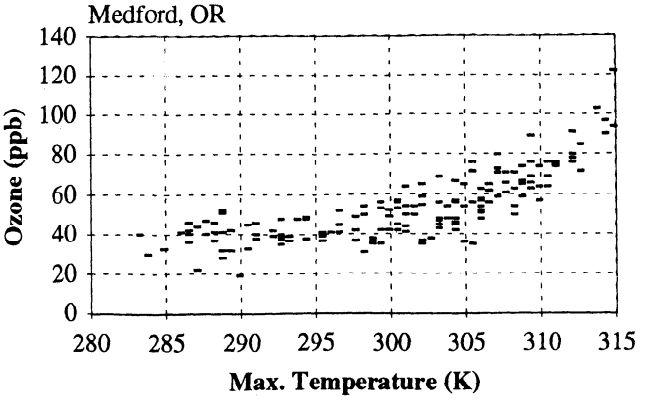

Figure 6f. Diurnal peak O_3 (ppb) at Medford, Oregon versus maximum temperature for April 1 to September 30, 1988, based on measurements from *EPA* [1991].

Table 2. Rates of Increase of Peak O_3 With Diurnal Maximum Temperature (ppb K^{-1}) For T<300 K and T>300 K, Based on Measurements for April 1-Sep. 30, 1988

Location	>T>300 K<			
	$\frac{\Delta O_3}{\Delta T}$	T-statistic[a]	$\frac{\Delta O_3}{\Delta T}$	T-statistic
		Urbanized Regions		
New York-New Jersey-Connecticut	1.5	(5.2)	8.8	(7.4)
Detroit	1.4	(6.4)	4.4	(6.3)
Atlanta	3.2	(4.2)	7.1	(5.9)
Phoenix	----[b]	----	1.4	(4.1)
Southern California	11.3	(8.9)	----[b]	----
		Nonurban Sites		
Williamsport, Pennsylvania	1.2	(5.0)	4.0	(7.4)
Saline, Michigan	0.8	(3.5)	3.1	(4.9)
Mammoth Cave, Kentucky	0.1	(0.3)	4.4	(7.3)
Kentucky, cleanest site[c]	0.3	(0.7)	3.4	(6.6)
Williston, North Dakota	0.2	(1.0)	0.8	(3.7)
Billings, Montana	0.1	(0.5)	0.7	(2.2)
Medford, Oregon	0.5	(2.6)	3.3	(13.7)

[a] The dependence of O_3 on temperature is statistically significant if t>1.6.

[b] The number of days with T<300 in Phoenix or T>300 in Los Angeles was too small to be included.

[c] O_3 values were chosen from the Kentucky site with the lowest peak O3 on each day.

The O_3-temperature curves from simulations (Figure 2) have been superimposed on the observed O_3 for Detroit and for a site in rural Michigan in Figure 6. Simulated O_3 falls within the range of observed O_3 versus temperature but there are significant differences between the simulated and observed patterns. The observed rate of increase of O_3 with temperature is approximately 2 times higher than the simulated rate of increase at both locations. Simulations also predict a continuous rise of O_3 with temperature with no change in behavior for temperatures above and below 300 K. These differences between simulated and observed patterns may be partly due to meteorological factors, since warm temperatures in the eastern United States are associated with bright sunshine, light winds, and stagnant circulation patterns which are conducive to formation of O_3 [*Mukammal et al.*, 1982]. Recently *Jacob et al.* [1993] reported that atmospheric circulation represents a significant component of O_3-temperature correlations in simulations with meteorology derived from a general circulation model. It has also been suggested that anthropogenic emissions increase at high temperatures, associated with the performance of automobiles [*EPA*, 1989; *Stump et al.*, 1992] or with high electricity loads.

The PAN-temperature curves shown in Figure 4a can also be compared with observations at Longwoods, Ontario, reported by *Brice et al.* [1988]. Observed concentrations of PAN ranged from 0.5 to 3 ppb with a seasonal maximum in spring and fall. These observations qualitatively agree with the simulated 1-2 ppb for PAN in rural Michigan with a maximum at 283° K. *Wunderli and Gehrig* [1991] report a very different pattern at two sites near Zurich, Switzerland, with much lower concentrations of PAN (0.2-1.2 ppb) and a minimum rather than a maximum at intermediate temperatures (273°-283° K diurnal average). They attribute this minimum to seasonal cloudiness during spring and fall rather than to direct dependence of PAN on temperature. *Wunderli and Gehrig* [1991] also report a strong correlation between peak concentrations of PAN and O_3. This correlation may reflect common antecedents of PAN and O_3 or it may reflect the photochemical link between the two [see *Sillman et al.*, 1990a].

Simulated NO_x (~0.4 ppb at 2 p.m.) is significantly lower than the median NO_x concentration (0.9 ppb) reported by *Buhr et al.* [1990] at a rural site in Pennsylvania. This discrepancy could be due to the heavy concentration of sources of NO_x in western Pennsylvania.

5. Results of Global Simulations

Recently, there has been great interest in identifying export of ozone and precursors from polluted continental regions and its impact on the free troposphere. The above analysis demonstrates that export varies greatly with temperature. The following calculations with the one-dimensional global model described in (Section 2) above show that ozone-temperature relationships in the free troposphere are fundamentally different from the identified relationship in polluted locations.

Global-scale calculations have been performed for three scenarios: a base case with a temperature profile equal to the U.S. Standard Atmosphere (surface temperature, 285° K), a case with temperatures throughout the troposphere increased by 5° K, and a case with a surface temperature of 303° K in the model subsection representing the polluted boundary layer. The second scenario is similar to the high-temperature cases examined by *Callis et al.* [1983]. The third scenario is designed to investigate the impact of regional pollution events associated with high temperatures on the free troposphere. While this does not represent a realistic scenario, it may be used to establish limits on the global impact of air pollution events, which can otherwise be represented only in three-dimensional global models with de-

Table 3. Concentrations, Sources and Sinks for O_3 and Reactive Nitrogen (10^3 molecules cm^{-3} s^{-1}) At 70 kpa from Global Simulation With (1) Standard Temperature Distribution (285 K At 100 kpa), (2) Temperature Increased by 5 K at All Altitudes and [H_2o] Increased to Maintain 50% Relative Humitity, and (3) Standard Temperature Distribution and Temperature in the Subsection Representing the Boundary Layer in Polluted Environments Increased by 15 K

	Standard Temperature	Increased Temperature	Warm Boundary Layer
		Concentrations	
NO_x	19.3	20.8	17.6
PANs	192.	181.	157.
HNO_3	168.	181.	160.
RNO_3	93.	80.	89.
O_3 (ppb)	43.4	40.8	42.5
		In Situ Emissions	
NO_x	1.7	1.7	1.7
		Net Transport	
NO_x	1.7	1.9	1.4
PANs	-1.0	-0.9	-1.3
HNO_3	3.8	3.8	2.9
RNO_3	1.0	1.0	1.0
O_3	109.	123.	116.
		Deposition	
HNO_3	7.2	7.6	6.9
		Photochemistry	
NO_x ->PANs	5.1	4.8	4.6
PANs->NO_x	4.0	3.9	3.3
NO_x ->HNO_3	4.7	5.2	4.1
HNO3 -> NO_x	1.2	1.3	1.1
NO_x -> RNO_3	1.3	1.2	1.2
RNO_3 -> NO_x	2.4	2.2	2.2
O_3 source	255.	279.	231.
O_3 sink	370.	416.	359.

Units are 10^3 molecules $cm^{-3}sec^{-1}$ or as Specified.

tailed meteorology. H_2O concentrations are adjusted in each simulation to maintain 50% relative humidity.

Results (Table 3) show concentrations for O_3 and reactive nitrogen that are typical of previous calculations with one- and two-dimensional models [e.g. *Fishman and Crutzen*, 1977; *Logan*, 1985; *Bruhl and Crutzen*, 1988]. Calculated OH and HO_2 ($4.1x10^6$ and $3.5x10^8$ cm^{-3} at 1400 at 70 kPa) are also consistent with prior calculations [e.g. *Logan et al.*, 1981]. The concentration of PAN (130 ppt at 70 kPa) is consistent with recent simulations [*Kanakidou et al.*, 1991; *Kasting and Singh*, 1986] which report PAN concentrations of ~100 ppt and observations in the 100-200 ppt range [*Ridley et al.*, 1990; *Singh et al.*, 1990; *Fahey et al.*, 1986]. However, the concentration of peroxypro-pionylnitrate (PPN) (40 ppt at 70 kPa) is higher than observed [*Singh et al.*, 1986] by a factor of 4. Simulated PPN is also higher than in the models of *Kanakidou et al.* [1991] and *Kasting and Singh* [1986], although this difference is apparently due to our assumption of a profile of VOC emissions in which >C4 alkanes predominate. The contrast between simulated and observed PPN may reflect shortcomings in the either the chemistry or the atmospheric composition of >C4 alkanes. Alternately, the rate of the reaction of OH with PPN, currently projected from the known rate of OH with PAN [*Kasting and Singh*, 1986], could be in error. Alkyl nitrates are also unusually high for reasons discussed in connection with the regional-scale simulations.

Simulated concentrations of NO_x in the free troposphere (19 ppt at 70 kPa) are comparable with the results of several recent models [*Penner et al.*, 1991; *Ehhalt et al.*, 1992; *Kanakidou et al.*, 1991] but are significantly lower than observed concentrations (34-65 ppt) [*Carroll et al.*, 1990]. Simulated concentrations of HNO_3 (170 ppt) are also comparable with the results of *Penner et al.* [1991] and *Ehhalt et al.* [1992], but are somewhat higher than observed values of ~100 ppt [*LeBel et al.*, 1990; *Huebert et al.*, 1990]. These discrepancies are a recurrring problem with global models, although some older models [*Logan et al.*, 1981; *Thompson et al.*, 1982; *Stewart et al.*, 1983; *Kasting and Singh*, 1986] have obtained NO_x and HNO_3 concentrations that were closer to observations. An additional dimension of the problem is the ratio HNO_3:NO_x, which is 9:1 in the model but 3:1 in

observations [*LeBel et al.*, 1990; *Huebert et al.*, 1990]. The simulated PAN:NO_X ratio (10:1) is also significantly higher then the ratios observed by *Ridley et al.* [1990], although this appears to be the result of erroneous NO_X rather then erroneous PAN.

Table 3 also shows rates for net vertical transport, emissions, surface deposition and photochemical transformations affecting NO_y and O_3 at 70 kPa for the three scenarios. The source of odd nitrogen in the standard scenario is dominated by vertical transport of HNO_3 (3.8E3 $cm^{-3}s^{-1}$ versus 1.7E3 $cm^{-3}s^{-1}$ for NO_X transport and 1.8E3 $cm^{-3}s^{-1}$ for in situ emission of NO_X). The model also shows photochemical conversion of NO_X to HNO_3 (4.7E3 $cm^{-3}s^{-1}$) balanced by HNO_3 deposition (7.2E3 $cm^{-3}s^{-1}$), but photochemical production of NO_X via HNO_3+OH and HNO_3+hν reactions is comparable to the NO_X sources from transport and in situ emissions. PAN chemistry results in net photochemical formation of PAN which is balanced by net downward flux to warmer regions of the atmosphere where PAN removal via thermal decomposition is faster, as in the work of *Kasting and Singh* [1986]. The photochemical source and sink for O_3 (2.2E10 $cm^{-3}s^{-1}$ and 3.2E10 $cm^{-3}s^{-1}$, respectively) are both larger than net transport (9.4E9 $cm^{-3}s^{-1}$), as is common in models of this type [e.g. *Chameides and Walker*, 1983].

Calculations based on a 5° increase in temperature throughout the troposphere result in a 6% decline in O_3. This change in O_3 is somewhat smaller then the equivalent change by *Callis et al.* [1983] which did not include PAN chemistry. The in situ photochemical sink for O_3 increases by 9% as a result of higher H_2O in the scenario, but this is partially offset by an increased photochemical source associated with higher NO_X. The increased NO_X at 70 kPa in the scenario is associated with smaller net conversion from NO_X to PAN and increased transport of NOx from lower altitudes, both associated with the higher PAN decomposition rate. Without PAN chemistry the increased temperature and H_2O would cause a decrease in NOx rather than an increase.

When the calculation is repeated with a warm polluted layer (scenario 3) the result is a slight (2%) decrease in O_3 in the remote and midtroposphere. This decrease occurs despite the fact that export of O_3 from the polluted subregion has increased. As shown in Table 3, changes associated with this scenario include increased export of HNO_3 to the free troposphere and decreased export of NO_X, PAN, and total NO_y. The latter is associated with the shorter lifetime of PAN in the warm polluted layer. NO_X in the remote troposphere decreases by ~10% and photochemical production of O_3 decreases by a similar amount. As shown in Table 3, the increased source of O_3 at 70 kPa due to transport, associated with increased export from the polluted boundary layer, is more than compensated by decreased in situ photochemical production of O_3, associated with reduced NO_X. The warm boundary layer is associated with decreased upward transport of NO_X and RNO_3 at 70 kPa and increased downward transport of PAN, resulting in lower NO_X. This result suggests emission of anthropogenic precursors affects the global budget for O_3 to an equal or even greater extent when localized high O_3 does not occur. The small decrease in O_3 in the warm boundary layer scenario is associated with the tendency for more efficient production of O_3 from NO_X under low-NOx conditions, as discussed by *Liu et al.* [1987], *Lin et al.* [1988] and *Chatfield and Delany* [1990].

6. Conclusions

Results of the modeling exercise and accumulated observations confirm the widely acknowledged view that O_3 concentrations in polluted environments are closely linked to temperature. We have shown that a significant portion of the O_3-temperature relationship is associated with temperature-dependent photochemical rate constants, in particular with the removal rate for PAN and its homologues. PAN chemistry appears to have an equal or greater impact than the more obvious causes of the temperature dependence, i.e., insolation, H_2O, or increased emission of isoprene. However, the pattern of observations from both urban and rural locations suggests that the relationship between O_3 and temperature is significantly stronger than the models would predict.

The unexplained portion of the observed O_3-temperature correlations could be due to the relation between stagnant atmospheric circulation and temperature, as suggested by *Jacob et al.* [1993] or with correlations between temperature and anthropogenic emissions. There is evidence to suggest that increased temperature is associated with increased emission of VOC, via automobile performance [*EPA*, 1989; *Stump et al.*, 1992], but the correlation between NO_X and temperature is more ambiguous [*Cardelino and Chameides*, 1990]. A correlation between NO_X emissions and temperature would be especially important with regard to rural O_3 concentrations, which have been linked to NO_X rather then to VOC [*Sillman et al.*, 1990a; *McKeen et al.*, 1991]. Further exploration of the relationship between NO_X and temperature should be possible by making use of existing NO_X and NO_y observations [*Buhr et al.*, 1990] in combination with a regional-scale model.

Results of global calculations illustrate two important features. First, in situ chemistry in the free troposphere is likely more important than direct transport of O_3 from polluted regions, although transport from polluted regions may be locally important [*Fishman et al.*, 1990]. Second, export of precursors (especially reactive nitrogen) from polluted regions has an equal or even greater impact on O_3 in the remote troposphere even when meteorological conditions prevent the formation of locally high O_3 concentrations in the polluted region. Export of PAN from polluted regions effectively replaces export of O_3 when temperatures are low. A thorough analysis of the role of export from polluted regions on global O_3 requires the use of a three-dimensional global model.

Acknowledgements. Discussions with Hiram Levy at NOAA Geophysical Fluid Dynamics Laboratory, Princeton, and with Stuart McKeen, Martin Buhr and Steven Berdman at NOAA Aeronomy Laboratory, Boulder, were very helpful in the preparation of this manuscript. This work was supported by the National Science Foundation (ATM-9014238).

References

Brice, K. A., J. W. Bottenheim, K. G. Anlauf, and H. A. Wiebe, Long-term measurements of atmospheric peroxyacetylnitrate (PAN) at rural sites in Ontario and Nova Scotia: Seasonal variations and long-range transport, *Tellus 40(B)*, 408-425, 1988.

Bruhl, C., and P. J. Crutzen, Scenarios of possible changes in atmospheric temperatures and ozone concentrations due to man's activities, estimated with a one-dimensional coupled photochemical climate model, *Clim. Dyn.*, 2, 173-203, 1988.

Buhr, M. P., D. D. Parrish, R. B. Norton, F. C. Fehsenfeld. R. E. Sievers, and J. M. Roberts, Contributions of organic nitrates to the total reactive nitrogen budget at a rural eastern U.S. site, *J. Geophys. Res.*, *95*, 9809-9816, 1990.

Callis, L. B., M. Natarajan, and R. E. Boughner, On the relationship between the greenhoues effect, atmospheric photochemistry, and species distribution, *J. Geophys. Res.*, 88, 1401-1426, 1983.

Cardelino, C. A., and W. L. Chameides, Natural hydro-carbons, urbanization, and urban ozone, *J. Geophys. Res.*, *95*, 13,971-13,979, 1990.

Carroll, M. A., et al., Aircraft measurements of NO_X over the eastern Pacific and continental United States and implications for ozone production, *J. Geophys. Res.*, *95*, 10,205-10,234, 1990.

Chameides, W. L., and J. C. G. Walker, A photochemical theory of tropospheric ozone, *J. Geophys. Res.*, *78*, 8751-8760, 1973.

Chatfield, R. B., and A. C. Delany, Convection links biomass burning to increased tropical ozone: However, models will tend to overpredict O_3, *J. Geophys. Res.*, *95*, 18,473-18,488, 1990.

Clark, T. L., and T. R. Karl, Application of prognostic meteorological variables to forecasts of daily maximum one-hour ozone concentrations in the northeastern United States, *J. Appl. Meteorol.*, *21*, 1662-1671, 1982.

DeMore, W. B., J. J. Margitan, M. J. Molina, R. T. Watson, D. M. Golden, R. F. Hampson, M. J. Kurylo, C. J. Howard, and A. R. Ravishankara, Chemical kinetics and photo-chemical data for use in stratospheric modeling, *Jet Propul. Lab. Publ. 85-37*, Calif. Inst. of Technol., Pasadena, Calif., 1985.

DeMore, W. B., S. P. Sander, D. M. Golden, R. F. Hampson, M. J. Kurylo, C. J. Howard, A. R. Ravishankara, C. E. Kolb, and M. J. Molina, Chemical kinetics and photochemical data for use in stratospheric modeling, *JPL Publ. 92-20*, Jet Prop. Labo., NASA, 1992.

Dignon, J., and J. A. Logan, Biogenic emissions of isoprene: A global inventory, *Eos Trans. AGU*, *71*, 1260, 1990.

Ehhalt, D. H., F. Rohrer, and A. Wahner, Sources and distribution of NO_X in the upper troposphere at northern midlatitudes, *J. Geophys. Res.*, *97*, 3725-3738, 1992.

Environmental Protection Agency (EPA), Development of the 1980 NAPAP emissions inventory, *EPA-600/7-86-057a*, Research Triangle Park, N. C., 1986.

Environmental Protection Agency, Users guide to mobile-IV, *EPA-AA-TEB-89-01*, Office of Mobile Sources, Ann Arbor, Mich, 1989.

Environmental Protection Agency, *Aerometric Information Retrieval System* (AIRS), Research Triangle Park, N. C., 1991.

Fahey, D. W., G. Hubler, D. D. Parrish, E. J. Williams, R. B. Norton, B. A. Ridley, H. B. Singh, S. C. Liu, and F. C. Fehsenfeld, Reactive nitrogen species in the troposphere: Measurements of NO, NO_2, HNO_3, particulate nitrate, peroxyacetylnitrate (PAN), O_3, and total reactive odd nitrogen (NO_y) at Niwot Ridge, Coloado, *J. Geophys. Res.*, *91*, 9781-9793, 1986.

Fishman, J., and P. J. Crutzen, A numerical study of tropospheric photochemistry using a one-dimensional model, *J. Geophys. Res.*, *82*, 5897-5905, 1977.

Fishman, J., C. E. Watson, J. C. Larsen, and J. A. Logan. Distribution of tropospheric ozone determined from satellite data. *J. Geophys. Res.*, *95*, 3599-3619, 1990.

Flowers, E. C., R. A. McCormick, and K. R. Kurfis, Atmospheric turbidity over the United States, 1961-1966, *J. Appl. Meteorol.*, *8*, 955-962, 1969.

Foltman, R., Detroit Edison Mesoscale and Measurements Network, Detroit Edison Company, 1988.

Hameed, S., R. D. Cess, and J. S. Hogan, Response of the global climate to changes in atmospheric chemical composition due to fossil fuel burning, *J. Geophys Res.*, *85*, 7537-7545, 1980.

Heffter, J. L., Air Resources Laboratories atmospheric transport and dispersion model (ARL-ATAD), *NOAA Tech. Memo. ERL-ARL-81*, 17 pp., Air Resour. Lab., Silver Spring, M., 1981.

Holtzworth, G. C., Estimates of mean mixing depths in the contiguous United States, *Mon. Weather Rev.*, *92*, 235-247, 1974.

Huebert, B. J., et al., Measurements of the nitric acid to NO_X ratio in the troposphere, *J. Geophys. Res.*, *95*, 10,193-10,198, 1990.

Jacob, D. J., B. G. Heikes, R. R. Dickerson, R. S. Artz and W. C. Keene. Evidence for a seasonal transition from NO_X- to hydrocarbon-limited ozone production at Shenandoah National Park, Virginia. Submitted to *J. Geophys. Res.*, 1993a.

Jacob, D. J., J. A. Logan, G. M. Gardner, R. M. Yevich, C. M. Spivakowsky, S. C. Wofsy, S. Sillman, and M. J. Prather, Factors regulating ozone over the United States and its export to the global troposphere, *J. Geophys. Res.*, *98*, 14,817-14,826, 1993.

Jacob, D. J., and S. C. Wofsy, Photochemistry of biogenic emissions over the Amazon forest, *J. Geophys. Res.*, *93*, 1477-1486, 1988.

Jacob, D. J., L. W. Horowitz, J. W. Munger, B. G. Heikes, R. R. Dickerson, R. S. Artz, and W. C. Keene, Seasonal transition from NO_X- to hydrocarbon-limited ozone production over the eastern United States in September, *J. Geophys. Res.*, in press, 1995.

Kanakidou, M., H. B. Singh, K. M. Valentin, and P. J. Crutzen, A two-dimensional study of ethane and propane oxidation in the troposphere, *J. Geophys. Res.*, *96*, 15,395-15,414, 1991.

Kasting, J. F., and H. B. Singh, Nonmethane hydrocarbons in the troposphere: Impact on the odd hydrogen and odd nitrogen chemistry, *J. Geophys. Res.*, *91*, 13,239-13,256, 1986.

Kelly, N. A., M. A. Ferman, and G. T. Wolff, The chemical and meteorological conditions associated with high and low ozone concentrations in southeastern Michigan and nearby areas of Ontario, *J. Air Pollut. Control Assoc.*, *36*, 150, 1986.

Kleinman, L. I., Photochemical formation of peroxides in the boundary layer, *J. Geophys. Res.*, *91*, 10,889-10,904, 1986.

Kleinman, L. I., Seasonal dependence of boundary layer peroxide concentration: The low and high NO_X regimes, *J. Geophys. Res.*, *96*, 20,721-20,734, 1991.

Lamb, B., A. Guenther, D. Gay, and H. Westberg, A national inventory of biogenic hydrocarbon emissions, *Atmos. Environ.*, *21*, 561-568, 1987.

LeBel, P. J., B. J. Huebert, H. I . Schiff, S. A. Vay, S. E. Van Bramer, and D. R. Hastie, Measurements of tropospheric nitric acid over the western United States and northeastern Pacific Ocean, *J. Geophys. Res.*, *95*, 10,199-10,204, 1990.

Lin, X., M. Trainer, and S. C. Liu, On the nonlinearity of tropospheric ozone, *J. Geophys Res.*, *93*, 15,879-15,888, 1988.

Liu, S. C., D. Kley, M. McFarland, J. D. Mahlman, and H. Levy, On the origin of tropospheric ozone, *J. Geophys. Res.*, *85*, 7546-7552, 1980.

Liu S. C., M. Trainer F. C. Fehsenfeld, D. D. Parrish, E. J. Williams, D. W. Fahey, G. Hubler, and P. C. Murphy, Ozone production in the rural troposphere and implications for regional and global ozone distributions, *J. Geophys Res.*, *92*, 4191-4207, 1987.

Logan, J. A., Nitrogen oxides in the troposphere: Global and regional budgets, *J. Geophys Res.*, *88*, 10,785-10,807, 1983.

Logan, J. A., Tropospheric ozone: Seasonal behavior, trends, and anthropogenic influence, *J. Geophys. Res.*, *90*, 10,463-10,482, 1985.

Logan, J. A., Ozone in rural areas of the United States, *J. Geophys. Res.*, *94*, 8511-8532, 1989.

Logan, J. A., M. J. Prather, S. C. Wofsy, and M. B. McElroy, Tropospheric chemistry: A global perspective, *J. Geophys. Res.*, *86*, 7210-7254, 1981.

Lurmann, F. W., A. C. Lloyd, and R. Atkinson, A chemical mechanism for use in long-range transport/acid deposition computer modeling, *J. Geophys. Res.*, *91*, 10,905-10,936, 1986.

Madronich, S., Photodissociation in the atmosphere; 1, Actinic flux and the effect of ground reflections and clouds, *J. Geophys. Res. 92*, 9740-9752, 1987.

Matthews, E., Global vegetation and land use: New high-resolution data bases for climate studies, *J. Clim. Appl. Meteorol.*, *22*, 474, 1983.

McKeen, S. A., E-Y. Hsie, and S. C. Liu, A study of the dependence of rural ozone on ozone precursors in the eastern United States. *J. Geophys. Res.*, *96*, 15377-15394, 1991.

Mukammal, E. I., H. H. Neumann and T. J. Gillespie, Meteorological conditions associated with ozone in southwestern Ontario, Canada, *Atmos. Environ., 16*, 2095-2106, 1982.

Mukammal, E. I., H. H. Neumann, and T. R. Nichols, Some features of the ozone climatology of Ontario, Canada and possible contributions of stratospheric ozone to surface concentrations, *Arch. Meteorol. Geophys. Bioklimatol., Ser. A., 34*, 179-211, 1985.

Paulson, S. E. and J. H. Seinfeld, Development and evaluation of a photooxidation mechanism for isoprene, *J. Geophys. Res., 97*, 20,703-20,715, 1992.

Penner, J. E., P. S. Connell, D. J. Wuebbles, and C. C. Covey, Cimate change and its interactions with air chemistry: Perspectives and research needs, EPA report under interagency agreement DW89932676-01-1, Lawrence Livermore National Laboratory, Calif., 1988.

Penner, J. E., C. S. Atherton, J. Dignon, S. J. Ghan, J. J. Walton, and S. Hameed, Tropospheric nitrogen: A three-dimensional study of sources, distributions, and deposition, *J. Geophys. Res. 96*, 959-990, 1991.

Prather, M. J., Numerical advection by conservation of second-order moments, *J. Geophys Res., 91*, 6671-6681, 1986.

Ramanathan, V., et al., Climate-chemical interactions and effects of changing atmospheric trace gases, *Rev. Geophys., 25*, 1441-1482, 1987.

Ridley, B. A., et al., Ratios of peroxyacetyl nitrate to active nitrogen observed during aircraft flights over the eastern Pacific oceans and continental United States, *J. Geophys Res., 95*, 10179-10192, 1990.

Sillman, S., J. A. Logan, and S. C. Wofsy, The sensitivity of ozone to nitrogen oxides and hydrocarbons in regional ozone episodes, *J. Geophys. Res., 95*, 1837-1851, 1990a.

Sillman, S., J. A. Logan, and S. C. Wofsy, A regional-scale model for ozone in the United States with a subgrid representation of urban and power plant plumes, *J. Geophys. Res., 95*, 5731-5748, 1990b.

Sillman, S., and P. J. Samson, Nitrogen oxides, regional transport and ozone air quality: Results of a regional-scale model for the midwestern United States, *Water Air Soil Pollut., 67*, 117-132, 1993.

Singh, H. B., L. J. Salas, and W. Viezee, Global distribution of peroxyacetyl nitrate, *Nature, 321*, 588-591, 1986.

Singh, H. B., et al., Peroxyacetyl nitrate measurements during CITE 2: Atmospheric distribution and precursor relationships, *J. Geophys. Res., 95*, 10,163-10,179, 1990.

Smolarkiewicz, P. K., A simple positive definite advection scheme with small implicit diffusion, *Mon. Weather. Rev., 111*, 479-486, 1983.

Stewart, R. W., S. Hameed, and G. Matloff, A model study of the effects of intermittent loss on odd nitrogen concentrations in the lower troposphere, *J. Geophys. Res., 88*, 10,697-10,707, 1983.

Stump, F. D., K. T. Knapp, W. D. Ray, R. Snow and C. Burton, The composition of motor vehicle organic emissions under elevated temperature summer driving conditions (75 to 105°F), *J. Air Waste Manage. Assoc., 42*, 152-158, 1992.

Thompson, A. M., and R. J. Cicerone, Clouds and wet removal as causes of variability in the trace-gas composition of the marine troposphere, *J. Geophys. Res., 87*, 8811-8826, 1982.

Thompson, A. M., and D. H. Lenschow, Mean profiles of trace reactive species in the unpolluted marine surface layer, *J. Geophys. Res., 89*, 4788-4796, 1984.

Thompson, A. M., M. A. Hurley, and R. W. Stewart, Perturbations to tropospheric oxidants, 1985-2035, 1, calculations of ozone and OH in chemically coherent regions, *J. Geophys. Res., 95*, 9829-9844, 1990.

Trainer, M., et al., Correlation of ozone with NO_y in photochemically aged air, *J. Geophys. Res., 98*, 2917-2926, 1993.

van Ulden, A. P., and A. A. M. Holtslag, Estimation of atmospheric boundary-layer parameters for diffusion applications, *J. Clim.Appl. Meteorol., 24*, 1196-1207, 1985.

Vukovich, F. M., W. D. Bach, B. W. Crissman, and W. J. King, On the relationship between high ozone in the rural surface layer and high pressure systems, *Atmos. Environ., 11*, 967-983, 1977.

Wunderli, S., and R. Gehrig, Influence of temperature on formation and stability of surface PAN and ozone. A two year field study in Switzerland, *Atmos. Environ., 25(A)*,1599-1608, 1991.

P. J. Samson and S. Sillman, Department of Atmospheric, Oceanic and Space Sciences, University of Michigan, Ann Arbor, MI 48109-2143.

(Received June 8, 1992; revised August 4, 1994;
accepted August 15, 1994.)